J. Chem. Sci. Vol. 129, No. 3, March 2017, pp. 353–358.
DOI 10.1007/s12039-017-1234-1

REGULAR ARTICLE

Hydrodechlorination of $(CH_3)_3SiCHCl_2$ over Pd, Ni, Co and Fe supported on AlF_3

RATEB HINA*, ISAM ARAFA and OMAR ENNAB

Department of Chemistry, Jordan University of Science and Technology, P.O. Box 3030, Irbid 22110, Jordan
Email: rhhina@just.edu.jo

MS received 9 December 2016; revised 18 December 2016; accepted 7 January 2017

Abstract. Gas phase hydrodechlorination (HDC) process of $Me_3SiCHCl_2$ was studied in a flow reactor at 200°C using a 2% metal loading (w/w) of four different monometallic catalysts (Pd/AlF_3, Ni/AlF_3,Co/AlF_3 and Fe/AlF_3). The catalysts were prepared by sol-gel method and structurally examined by BET method, FT-IR and XPS techniques. The XPS technique showed that Ni^{II}, Fe^{III} and Co^{III} exist as oxides. The major products in the HDC process of $Me_3SiCHCl_2$ were identified by GC and GC-MS and found to include Me_3SiCH_2Cl, Me_3SiCl, and Me_4Si. The effect of these catalysts on the quantitative conversion, selectivity and conversion rates are reported.

Keywords. Hydrodechlorination; chloroorganosilane; Aluminium Fluoride; dichloromethyl trimethylsilane.

1. Introduction

Catalytic hydrodechlorination process (HDC) of chlorinated organic compounds over monometallic (Pd, Pt, Fe, Ni, Zn, etc.) and bimetallic (Pd-Fe, Pt-Au, Pd-Ag and Pd-Au, etc.) supported catalysts is well documented in the literature.[1–7] This process is widely employed in the elimination of alkyl and aryl chlorides such as CCl_4, CH_3Cl, CH_2Cl_2, CH_3Cl and $C_6H_xCl_{6-x}$ from organic waste. This reductive de-chlorination process was shown to proceed through a dissociative adsorption mechanism of the chlorinated organic substrates forming different intermediate species and consequently leading to the formation of C_1, C_2-C_5 coupled products and coke.[2–6,8,9]

Although, catalytic HDC process of chlorinated organic compounds was widely investigated, it is scarcely reported for chlorinated organosilane compounds such as R_xSiCl_{4-x} and R_3SiCH_2Cl.[10–15] In this respect, these chlorinated organosilanes belong to two different classes of organosilanes where, in the first class (≡Si-Cl) the -Cl is directly bonded to the silicon whereas in the second class (≡Si-CH_2-Cl), the -Cl is bonded to the carbon. Consequently, the Cl in ≡Si-Cl is readily hydrolysable whereas in the ≡Si-CH_2-Cl compounds it is stable towards hydrolysis and other chemical reagents. The first class of chlorinated organosilanes plays a key role in silicone polymer and silicon aerogel industries, while the second class provide essential precursors in electronic silicon industry, organosilicon chemistry, surface modification of commodity polymers, and chemical vapor deposition (CVD) in thin-film industry.[16–24]

The present work describes the HDC process of $Me_3SiCHCl_2$ precursor over 2% loading of monometallic Pd/AlF_3, Ni/AlF_3, Co/AlF_3 and Fe/AlF_3 catalysts in a flow reactor. The catalysts were prepared using sol-gel method and characterized by BET, infrared (FT-IR) and X-ray photoelectron spectroscopy (XPS). Gas-phase reaction of $H_2/Me_3SiCHCl_2$ mixture at constant temperature (200°C) was chosen as a model reaction to study the activity and selectivity of the obtained catalytic systems, as depicted below (Scheme 1). The products were identified using GC and GC-MS techniques.

2. Experimental

2.1 *Materials and methods*

All chemicals were of reagent grade and used as received without further purification. The hydrogen (99%) was purchased from International Industrial and Medical Liquid-Gas Co., Jordan. The reagents ($(CH_3)_3SiCHCl_2$, 96%; HF_{aq}, 48%; $PdCl_2$, 99%; $NiCl_2{\cdot}6H_2O$; $FeCl_2{\cdot}6H_2O$ and $CoCl_2{\cdot}6H_2O$) were obtained from Sigma-Aldrich Co. Absolute ethanol was supplied by Baker (BDH) and AlF_3 was obtained from Riedel-deHaen. All supported catalysts of 2% (w/w) metal loading used in this study Pd/AlF_3, Ni/AlF_3, Co/AlF_3 and Fe/AlF_3 were prepared by sol-gel method.

The internal surface area of the supported catalysts was measured by BET method using surface area analyzer (Quanta Chrom, Nova 2000 series, USA). All samples were degassed at 200°C for 16 h. The surface area (m^2/g)

*For correspondence

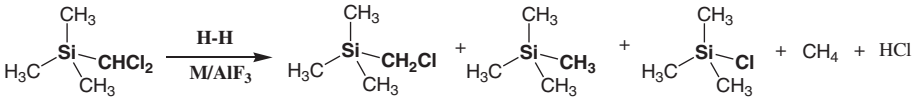

Scheme 1. Products of gas-phase catalytic reaction of $H_2/Me_3SiCHCl_2$ mixture at constant temperature (200°C).

was determined from the obtained isotherms of adsorption-desorption of nitrogen at 77 K. The FT-IR spectra of samples were recorded on Nicolet Impact 410-FT-IR spectrometer as KBr pellets. The samples were dried and placed in a desiccator at 20°C prior to the pellet preparation. Analysis of the prepared catalysts was also performed using X-Ray Photoelectron Spectroscopy (XPS). The samples were degassed prior to data collection on a Kratos Axis 165-X-Ray photoelectron spectrometer (monochromatic Al Kα radiation, 260 W; the samples were fixed to the sample holder using double-sided conductive copper tape, and charge neutralization was required to minimize charge build up on the surface; pressure of the system was below 5×10^{-8} torr. throughout the data collection).

2.2 *Preparation of Pd/AlF_3 catalyst by sol-gel method*

A calculated mass of anhydrous aluminum chloride salt ($AlCl_3$) was dissolved in ~40 mL of absolute ethanol in a plastic container. Immediately, the ethoxy derivative of aluminum, $Al(OEt)_3$ was observed to form accompanied by HCl evolution. The pH of the solution was adjusted to 1.0 by addition of HCl solution, then the required weight of $PdCl_2$ needed to prepare 2% (w/w) was suspended in a minimum amount of aqueous ethanol and added to the solution. The mixture was stirred and heated in a water bath to 60°C for 20 min. Excess volume of HF (~10 mL) solution was added slowly in a dropwise manner to the solution over a period of 30 min where a gel formed. The reaction was further heated (70°C, 3–4 h) to finally get a homogeneous gel. The ethanol was removed at ~80°C and the gel was dried overnight (100°C). The resulting dried gel was subjected to calcination in airflow (1 h, 100 mL/min, 200°C) followed by hydrogenation (4 h, 25 mL/min, 450°C). This procedure finally yielded 2% Pd/AlF_3 catalyst.

Similar procedure was adopted for the preparation of 2% Ni/AlF_3, Co/ AlF_3 and Fe/ AlF_3.

2.3 *HDC reaction*

The catalyst was placed on a glass fixed-bed reactor in which the catalyst was immobilized between two disks of glass wool. A mixture of H_2 and $Me_3SiCHCl_2$ vapor was introduced into the reactor tube at constant temperature by bubbling the H_2 gas through $Me_3SiCHCl_2$ liquid. The pressure ratio of $Me_3SiCHCl_2$:H_2 of $\leq$0.05 (atm) in the feed stream was controlled by adjusting the temperature of $Me_3SiCHCl_2$. The gas flow was controlled by using a mass flow controller (Cole Parmer) and manual flow meter controller (Gilmon, model 150 MM). The temperature of the reactor oven was measured by a thermocouple, and controlled ($\pm$1°C) using both a temperature controller (Antiness controls TCE) and AC transformer power supply. A suitable condenser was connected to the outlet of the reactor tube to condense the products of the reaction at $-$10°C. Each fresh catalyst (~0.50 g) sample was activated immediately before the reaction by flowing hydrogen gas at 450°C for 1 h, then cooling the catalyst to room temperature under helium gas flow. The vapor-phase HDC reaction was performed in a glass fixed-bed reactor in a flow system under a total pressure of 1 atm.

The composition of the reaction mixture was analyzed by GC (Shimadzu 2010) equipped with FID detector and DB-1701 capillary column (30 m length; 0.32 mm internal diameter; 0.25 μm film thickness, mid-polar stationary phase of 14% cyanopropyl-phenyl-86% polydimethylsiloxane). The flow rate of helium carrier gas was 1.78 mL/min. The detector and injector temperature was 200°C, while the temperature of the oven was controlled through the computer program of the GC. GC-MS instrument was used for further qualitative identification of products using Varian 450–GC, DB wax column (30 m length; 0.25 mm internal diameter; 0.25 μm film thickness; polar stationary phase polyethylene glycol) and mass spectrum (Varian 320-MSTQ). The flow rate of the carrier gas (helium) was 1 mL/min. The temperature of the detector, injector and oven were as mentioned above in the GC.

3. Results and Discussion

3.1 *Preparation of Catalysts and Characterization*

The investigated catalysts of 2% Pd, Ni, Fe, Co supported on AlF_3 were prepared by a standard sol-gel procedure and characterized by BET surface area, FT-IR and XPS techniques (Table 1). It is clear from the BET surface area that the 2% metal loaded catalysts exhibit smaller surface area (20–29 m^2/g) than that of the unloaded AlF_3 support (72 m^2/g).

The prepared catalytic systems were further examined by XPS spectroscopy, which is a powerful surface analytical technique.[25–27] Two important information can be gathered from this technique, namely, the actual loading percentage of the catalytic metals (Pd, Ni, Co, Fe) on the surface of the AlF_3 support and their oxidation states (Table 1). The XPS spectrum of the AlF_3 support displays one signal at 76.1 eV due to the Al (2p) and at 686.3 eV corresponding to the F (1s) (Table 1). These XPS peaks of the support were observed to shift to higher values of (76.6–76.9 eV) and (686.4–688.2 eV), respectively, for the metal loaded catalysts.

Table 1. BET surface area and XPS data for the prepared Pd, Ni, Fe and Co catalysts supported on AlF_3.

Catalyst	S_{BET} (m^2/g)	Binding Energy (eV)[a]	M%[b]	Catalytic site
AlF_3	72	**Al** 2p (76.1); **F** 1s (686.3)	–	–
Pd/AlF_3	27	**Al** 2p (76.9); **F** 1s (687.1); **Pd** 3d(334.6, 339.7)	1.9	Pd^0
Ni/AlF_3	29	**Al** 2p (76.8); **F** 1s (688.2); **Ni** 2p(857.6, 862.0[c], 874.2); **O** 1s (533.2)	1.9	$Ni(OH)_2$
Fe/AlF_3	26	**Al** 2p (76.6); **F** 1s (686.4) **Fe** 2p(711.0-712.9, 717.2[c], 722.0, 738.7[c]); **O** 1s (530.1, 533.0)	1.5	$\alpha-Fe_2O_3$ $\alpha-FeOOH$
Co/AlF_3	20	**Al** 2p (76.6); **F** 1s (687.2); **Co** 2p(780,0, 785.1[c], 802.5); **O** 1s (531.9)	1.3	Co_2O_3

[a]Reference, C 1s (284.8 eV).
[b]The percentage of the experimentally loaded metal was 2%.
[c]Satallite peak.

These shifts are attributed to their interaction with the AlF_3 support (Table 1).

Analysis of XPS data of the Pd/AlF_3 catalyst shows that metallic Pd^0 is present with a loading percentage of 1.9% which is slightly less than the experimentally loaded value of 2%, Pd(3d) exhibits a well-separated spin-orbit doublets at 334.6 ($3d_{5/2}$) and 339.7 ($3d_{3/2}$) eV ($\Delta = 5.1$ eV) which is typical for metallic Pd^0, Figure 1 (See xpssimplified.com/knowledgebase.php, Thermoscientific, 2013). However, the XPS data of the other three catalysts show that they are present in the form of oxides / hydroxides ($Ni(OH)_2$, Co_2O_3, Fe_2O_3). The percent loading of Fe- and Co-oxides are lower than 2% while Ni-oxide is close to 2% (Table 1). Close examination of the observed XPS peak position and shape due to Ni($2p_{3/2}$) and ($2p_{1/2}$) doublets at 857.6 and 874.2 eV, respectively, ($\Delta = 16.6$ eV), shows that they correspond to $Ni(OH)_2$ rather than NiO. The XPS of Ni ($2p_{3/2}$ and $2p_{1/2}$) has a typical spin-orbit separation of 17.3 eV which is close to the observed value of 16.6 eV. The FT-IR spectrum of this catalyst contains peaks due to the stretching frequency of hydroxide ($\upsilon_{O-H} = 3420\,cm^{-1}$) in agreement with the formation of $Ni(OH)_2$, as observed in the XPS spectrum. Furthermore, the XPS due to the oxygen appears at 533.2 eV confirming the presence of hydroxide (OH) species. Generally, the XPS of Fe^{3+} compounds are high spin with multiplet-spin Fe(2p) spectra. The XPS analysis of the Fe(2p) signal of the catalyst shows a broad multiplet pattern centered at 711.0–712.9 eV region and a

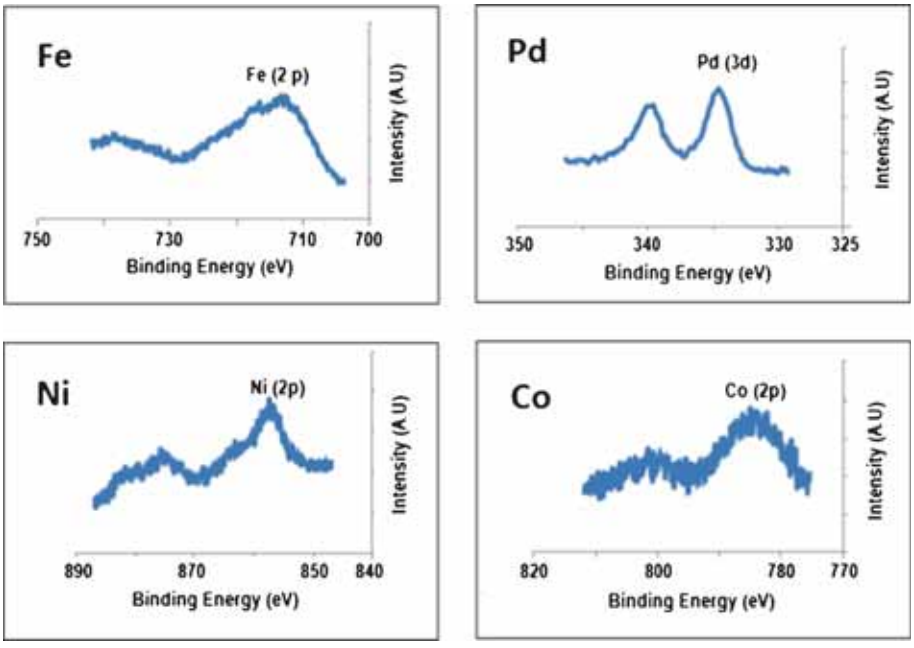

Figure 1. X-ray photoelectron spectra (XPS) for the prepared monometallic Pd, Fe, Co and Ni catalysts supported on AlF_3.

broad featureless shoulder at 722.0 eV ($\Delta = 11.0$ eV), which are attributed to the $Fe^{3+}(2p_{3/2})$ and $(2p_{1/2})$, respectively, of α-Fe_2O_3 and/or α-FeOOH. The commonly reported spin-orbit separation in the XPS of Fe^{3+} is about 13.0 eV which is close to the obtained value. However, the corresponding peak of the oxide appears at 530–533 eV which indicates the presence of two different type of oxygen due to oxide (530 eV) and hydroxide (533 eV). This observation suggests that oxygen is present as oxide and hydroxide which fits the presence of α-FeOOH. Furthermore, the FT-IR spectrum of this catalyst contains an unresolved broad peak due to the stretching frequency of hydroxide ($\upsilon_{O-H} = 3549–3350\,cm^{-1}$) in accordance with the formation of a hydroxide moiety (α-FeOOH) as deduced from the XPS spectrum.

Examination of the XPS spectrum of the cobalt catalyst shows a very broad Co(2p) peaks at 780.0 and 802.5 eV regions, assigned to $2p_{3/2}$ and $2p_{1/2}$ peaks of Co_2O_3 (Figure 1). The estimated spin-orbit of the XPS peaks of $\Delta = 22.5$ eV is higher than the commonly observed value of about 17 eV. This point may be the result of a strong interaction between the catalyst and its support. The appearance of XPS of the oxygen at 531.9 eV indicates the presence of oxide (Table 1). This conclusion is supported by the FT-IR data where no observable stretching frequency due to hydroxide was identified.

3.2 *Vapor phase HDC of $Me_3SiCHCl_2$ over M/AlF_3 catalysts (M = Pd, Ni, Fe, Co)*

The reaction rates are expressed as micromoles of reactant $Me_3SiCHCl_2$ converted per unit contact time (min) and mass (g) of the catalyst. Product selectivity is defined as the percentage ratio of the detected product C_i to the sum total amount of products: (% S) = 100 ($C_i/\Sigma\, C_i$).

All the HDC process rates quoted in this paper represent the steady-state values with no evidence of any catalyst deactivation throughout the course of the measurements. The reported values in Table 2 are the average of three trials with deviation of less than ±6%. The Lewis acidity of the AlF_3 support plays an important role in the desorption process of HCl formed during the HDC reaction and hence may affect the conversion rate and distribution of products. The HDC process of $Me_3SiCHCl_2$ over Pd, Ni, Fe, Co supported on AlF_3 catalysts yielded CH_4, different organosilane products identified as Me_3SiCH_2Cl, Me_3SiCl, Me_4Si and other coupled products (Me_3SiCH_2-CH_2SiMe_3 . . ...); see Table 2. It is clear from the data in Table 2 that the conversion rate over Pd/AlF_3 is much higher than those catalyzed over other transition metal catalysts, Ni/AlF_3, Fe/AlF_3 and Co/AlF_3. These metals show lower conversion rate. Inspection of the selectivity data in Table 2 shows that the Pd/AlF_3 catalyst exhibits high tendency for the formation of Me_3SiCH_2Cl while other transition metals comparably favor the formation of Me_3SiCl.

The plot in Figure 2 shows that the HDC rate increases linearly with increasing partial pressure of $Me_3SiCHCl_2$. These results suggest that the $Me_3SiCHCl_2$ was not adsorbed on the surface of the metal catalyst and the reaction mechanism can be represented by Eley-Rideal model[28] where the reaction takes place

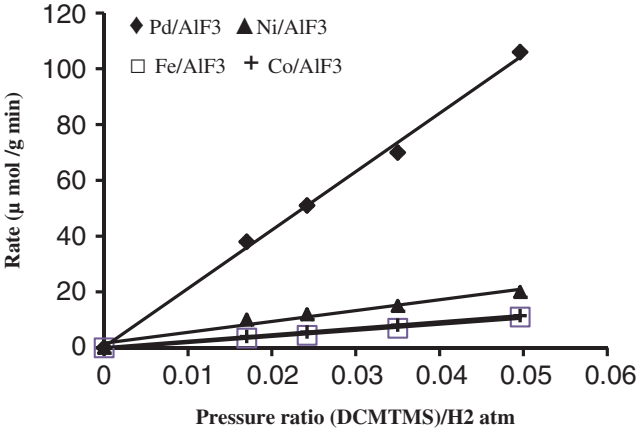

Figure 2. Rate of conversion as a function of pressure ratio of $Me_3SiCHCl_2$:H_2 over Pd, Ni, Fe and Co supported on AlF_3 at 200°C.

Table 2. Rate of conversion, percent conversion and percent selectivity for HDC process over M/AlF_3 where M = Pd, Ni, Fe, Co.

	Rate	Conversion[a]	Selectivity (%)[a]				
Catalyst	µmol/g min	%	CH_4 /CH_3Cl	Me_3SiCH_2Cl	Me_3SiCl	Me_3SiCH_3	Coupled[b]
Pd/AlF_3	106	11.6	10	49	15	10	16
Ni/AlF_3	20	5.5	25	22	34	6	13
Fe/AlF_3	11	3.5	33	18	38	4	7
Co/AlF_3	12	1.7	34	24	35	3	4

[a]Average of three trials; P ($Me_3SiCHCl_2$) / P(H_2) = 0.05 atm; 1 h on stream, 200°C.
[b]Coupled products such as Me_3SiCH_2-CH_2SiMe_3, ...

between the adsorbed hydrogen while $Me_3SiCHCl_2$ is present in the gas phase.

The effect of time–on–stream on the selectivity towards the formation of Me_3SiCH_2Cl and Me_3SiCl for all catalysts at 200°C is shown in Figures 3 and 4. The selectivity towards formation of both products showed linear and insignificant variation during the passivation time of ~2 h. However, the selectivity towards Me_3SiCl over Ni/AlF_3, Fe/AlF_3 and Co/AlF_3 are comparable (34–38%) and higher than Pd/AlF_3 catalyst (16%). Interestingly, Ni/AlF_3, Pd/AlF_3 catalysts exhibit higher tendency for the formation of coupled organosilane products than Fe/AlF_3 and Co/AlF_3.

It is clear from the selectivity data and the plots in Figures 3 and 4 that the Pd/AlF_3 catalyst favors the selective cleavage of C-Cl while the others, Ni, Fe and Co supported catalyst favor the cleavage of Si-C bond.

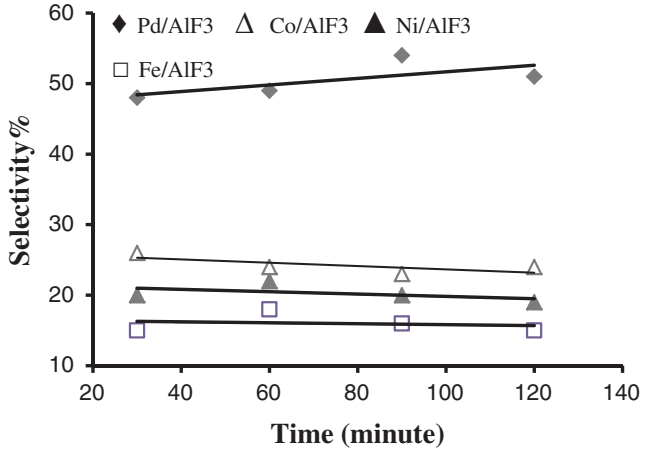

Figure 3. A plot of selectivity the monochloro product (Me_3SiCH_2Cl) as a function of time for HDC process of $Me_3SiCHCl_2$ over Pd, Ni, Fe and Co supported on AlF_3 at 200°C.

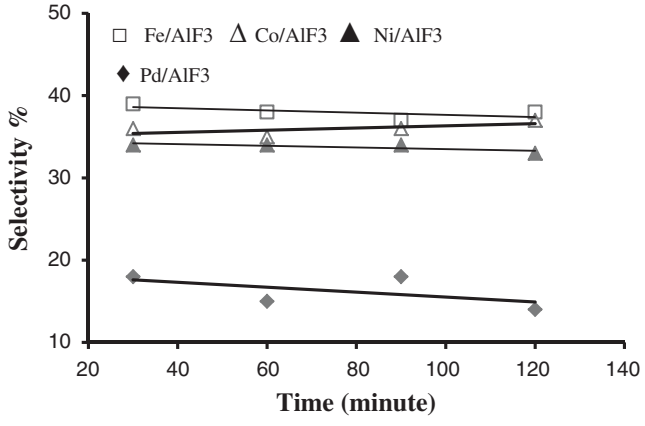

Figure 4. A plot of selectivity chlorosilane derivative (Me_3SiCl) as a function of time for HDC process of $Me_3SiCHCl_2$ over Pd, Ni, Fe and Co supported on AlF_3 at 200°C.

Furthermore, one can anticipate the formation of different reactive species including Cl^* (M-Cl) and H^* (M-H). The formation of Me_3SiCH_2Cl depends on the adsorbed reactive species Cl^* and H^* where the observation of high selectivity towards Me_3SiCH_2Cl on those catalysts may attributed to the long resident time of Cl^* and H^*-rich environment on the surfaces of the catalysts. The presence of Cl^* and H^* species may result in breaking of the Me_3Si-CH_2Cl, yielding Me_3SiCl, CH_3Cl, CH_4 and other silane derivatives including the coupled products. The formation of Me_3SiMe indicates the generation of CH_3^* adsorbed species. Different rate expressions and mechanisms have been proposed in literature specifically for catalytic HDC.[5,29,30] So, based upon the selectivity data, a proposed 3-step mechanism can be put forward:

$$Me_3SiCHCl_{2(g)} + M\text{-}H \rightarrow Me_3SiCH_2Cl_{(g)} + M\text{-}Cl \quad (1)$$

$$Me_3SiCH_2Cl_{(g)} + M\text{-}H + M\text{-}Cl \rightarrow Me_3SiCl_{(g)} + Me_3SiCH_{3(g)} + CH_3Cl_{(g)} + CH_{4(g)} + \text{Coupled Silanes} \quad (2)$$

$$M\text{-}Cl + H_{2(g)} \leftrightharpoons M\text{-}H + HCl_{(g)} \quad (3)$$

Step 1 involves the oxidative addition of $Me_3SiCHCl_2$ on the metal surface and its interaction with M-H and thus eliminating Me_3SiCH_2Cl into gas phase. Consequently, Me_3SiCH_2Cl gets adsorbed, undergoes similar process leading to the elimination of Me_3SiCl, Me_3SiCH_3, CH_3Cl and rest of the products into gas phase, as step 2. The surface is reversibly reduced by H_2 in step 3 and re-adsorption of HCl.[5,29] Each step 1, 2 and 3 can be described as having rate constants k_1, k_2 and k_3, respectively. The kinetic rate according to the proposed mechanism is given as follows:

$$\text{Rate} = k_1k_2\, P_R P_{H2}/(k_1P_R + k_2P_{H2} + k_3P_{HCl}) \quad (4)$$

P_R is the partial pressure of $Me_3SiCHCl_2$. This expression predicts a first order dependence with respect to $Me_3SiCHCl_2$. Under the reaction conditions employed in this study where $P_{Me_3SiCHCl_2} << P_{H2} >> P_{HCl}$, eq. 4 can be simplified as

$$\text{Rate} = k_1P_R \quad (5)$$

The data presented in Figure 4 and Table 2 reflects the dependence of reaction rate on partial pressure of $Me_3SiCHCl_2$. The experimentally determined rates increased with increasing partial pressure of $Me_3SiCHCl_2$ within the range of partial pressures used in this study.

4. Conclusions

Our findings show that unlike the HDC process of organic chlorides where the coupled products (C_2-C_5) are the major ones, the examined $Me_3SiCHCl_2$ gives a minor quantity of coupled products ($Me_3Si\mathbf{CH_2}$-$\mathbf{CH_2}SiMe_3$; $Me_3Si\mathbf{CHCl}$-$\mathbf{CHCl}SiMe_3$). The three major organosilane products are $Me_3Si\mathbf{CH_3}$, $Me_3Si\mathbf{CH_2Cl}$, and $Me_3Si\mathbf{Cl}$.

Acknowledgement

This work was financially supported by the Deanship of Research, Jordan University of Science and Technology, Irbid, Jordan.

References

1. Ahn B S, Lee S C, Moon D J and Lee B G 1996 A study on the hydrodechlorination reaction of dichlorodifluoromethane over PdAlF3 catalyst *J. Mol. Catal.* **106** 83
2. Karpiński Z, Bonarowska M and Juszczyk W 2014 Hydrodechlorination of tetrachloromethane over silica-supported palladium-gold alloys *PJCT* **16** 101
3. Bonarowska M, Malinowski A, Juszczyk W and Karpiński Z 2001 Hydrodechlorination of CCl_2F_2 (CFC-12) over silica-supported palladium–gold catalysts *Appl. Catal. B-Environ.* **30** 187
4. Bodnariuk P, Coq B, Ferrat G and Figueras F 1989 Carbon-chlorine hydrogenolysis over PdRh and PdSn bimetallic catalysts *J. Catal.* **116** 459
5. Sajiki H, Kume A, Hattori K, Nagase H and Hirota K 2002 Complete and truly catalytic degradation method of PCBs using Pd/C–Et3 N system under ambient pressure and temperature *Tetrahedron Lett.* **43** 7251
6. Coq B, Cognion J M, Figueras F and Tournigant D 1993 Conversion under hydrogen of dichlorodifluoromethane over supported palladium catalysts *J. Catal.* **141** 21
7. Coq B, Figueras F, Hub S and Tournigant D 1995 Effect of the metal-support interaction on the catalytic properties of palladium for the conversion of difluorodichloromethane with hydrogen: Comparison of oxides and fluorides as supports *J. Phys. Chem.-US* **99** 11159
8. Hina R H and Al-Fayyoumi R K 2004 Conversion of dichlorodifluoromethane with hydrogen over Pd/AlF_3 and Ru/AlF_3 prepared by sol–gel method *J. Mol. Catal. A-Chem.* **207** 27
9. He F and Zhao D 2008 Hydrodechlorination of trichloroethene using stabilized Fe-Pd nanoparticles: Reaction mechanism and effects of stabilizers, catalysts and reaction conditions *Appl. Catal. B-Environ.* **84** 533
10. Liu T, Wang X and Yin D 2015 Recent progress towards ionic hydrogenation: Lewis acid catalyzed hydrogenation using organosilanes as donors of hydride ions *RSC Adv.* **5** 75794
11. Ding S, Xiao W, Huang J, Deng S and Zhang N 2015 Hydrogenation of silicon tetrachloride to trichlorosilane over activated carbon-supported cobalt catalysts *Res. Chem. Intermediat.* **41** 5691
12. Kim B-h and Woo H-G 2004 Dehydrocoupling, redistributive coupling, and addition of main group 4 hydrides *Adv. Organomet. Chem.* **52** 143
13. Colin P, Jacquot R and Morel P 2002 U.S. Patent No. US 06384257. Washington, D.C.: U.S. Patent and Trademark Office
14. Drose J, Knott W and Wolfgram D 1999 U.S. Patent No. 5856548 A. Washington, D.C.: U.S. Patent and Trademark Office
15. Lee J Y, Lee W H, Park Y-K, Kim H Y, Kang N Y, Yoon K B, Choi W C and Yang O-B 2012 Catalytic conversion of silicon tetrachloride to trichlorosilane for a poly-Si process *Sol. Energ. Mat. Sol. C* **105** 142
16. Kalambettu A B, Rajangam P and Dharmalingam S 2012 The effect of chlorotrimethylsilane on bonding of nano hydroxyapatite with a chitosan polyacrylamide matrix *Carbohyd. Res.* **352** 143
17. Maloney R and Sakamoto J 2011 Large deformation of chlorotrimethylsilane treated silica aerogels *J. Non-Cryst. Solids* **357** 2059
18. Xu L-W 2011 Editorial [Hot Topic: Organosilicon-mediated Organic Synthesis/Organosilicon Chemistry (Guest Editor: Li Wen Xu)] *Curr. Org. Chem.* **15** 2742
19. Li X, Eustergerling B and Shi Y 2007 Mass spectrometric study of gas-phase chemistry in a hot-wire chemical vapor deposition reactor with tetramethylsilane *Int. J. Mass. Spectrom.* **263** 233
20. Inagaki N, Suzuki K and Nejigaki K 1983 Application of polymer films plasma polymerized in the tetramethylsilane/ammonia mixture to moisture sensor *J. Polym. Sci. Pol. Lett.* **21** 353
21. Malik S, Shah K J and Kartha K R 2010 Iodine-hexamethyldisilane (HMDS)-mediated anomerization of peracetylated 1, 2-trans-linked alkyl and aryl glycosides *Carbohyd. Res.* **345** 867
22. Durán-Galván M, Hemmer J R and Connell B T 2010 Synthesis of tertiary 1, 3-butadien-2-ylcarbinols from chromium-catalyzed addition of (4-bromobut-2-ynyl) trimethylsilane to ketones *Tetrahedron Lett.* **51** 5080
23. Parker B and Son D Y 2002 Silylated amino-triazines: New ligands with potential multi-coordination modes *Inorg. Chem. Commun.* **5** 516
24. Dhanya S, Kumar A and Naik P D 2007 Dissociation dynamics of chloromethyltrimethylsilane at 193 nm *Chem. Phys. Lett.* **438** 8
25. Turner N H and Schreifels J A 2000 Surface analysis: X-ray photoelectron spectroscopy and auger electron spectroscopy *Anal. Chem.* **72** 99
26. Wang B, Gao F and Ma H 2007 Preparation and XPS studies of macromolecule mixed-valent Cu (I, II) and Fe (II, III) complexes *J. Hazard. Mater.* **144** 363
27. Sun S and Wang A 2006 Adsorption kinetics of Cu (II) ions using N, O-carboxymethyl-chitosan *J. Hazard. Mater.* **131** 103
28. Weinberg W H 1996 Eley-Rideal surface chemistry: Direct reactivity of gas phase atomic hydrogen with adsorbed species *Acc. Chem. Res.* **29**(10) 479
29. Coq B, Ferrat G and Figueras F 1986 Conversion of chlorobenzene over palladium and rhodium catalysts of widely varying dispersion *J. Catal.* **101** 434
30. Keane M A and Murzin D Y 2001 A kinetic treatment of the gas phase hydrodechlorination of chlorobenzene over nickel/silica: Beyond conventional kinetics *Chem. Eng. Sci.* **56** 3185